Final Report

Small Business Innovation Research
Grant HI-9361914

A NEW APPROACH TO ESTIMATE DESIGN WIND CHARACTERISTICS FOR EXTENSIVE PRESSURE SYSTEM STORMS

Andrew Steckley
Peter J. Vickery
Lawrence A. Twisdale Jr.

Applied Research Associates, Inc.

Performing Division:
Southeast Division
6404 Falls of Neuse Road,
Suite 200
Raleigh, North Carolina 27615

Corporate Address
4300 San Mateo Blvd., NE
Suite A220
Albuquerque, New Mexico 87110

March 21, 1995
Prepared for
National Science Foundation
1800 G Street NW
Washington, D.C. 20550

This report has been recompiled from the original hardcopy report available from the National Science Foundation archives. It has been reformatted in order to preserve its content. Minor modifications have been made for clarification and typographical errors have been corrected.

PART II - ABSTRACT

This Phase I research investigated the viability of a new approach for estimating extreme wind characteristics for extensive pressure systems by deriving the wind field directly from a reconstructed pressure field. In the past, estimates of design windspeeds in the non-hurricane prone regions of the United States have been derived from historical records of windspeeds obtained from surface level anemometers. These surface level measurements are subject to errors produced by terrain effects, nearby structures and vegetation, changes in the mounting height of the instruments, and observation errors. They are taken only at a fixed anemometer stations and there is no first principle method to estimate winds at other locations.

In principle, it is possible to derive wind speeds and directons from the atmospheric pressure field, and historical records of atmospheric pressures at numerous stations throughout the United States are now available. The objectives of the present research were to investigate the viability of using these data to reconstruct large-scale pressure fields, to derive from these fields, the wind speeds and directions at arbitrary locations, and to compare the results of this approach to those of previous approaches which use anemometer records.

Automated pressure field reconstruction techniques were developed. Expressions for deriving the wind vectors from the pressure field were derived and comparisons of derived wind records and surface level measurements were made. Comparisons were also made between long-term wind statistics from both the new and conventional approaches. These comparison have clearly shown that the new approach is viable. Improvements in the techniques used have been identified and objectives for Phase II research have been suggested.

PART III - TECHNICAL INFORMATION

Software Developed

(i) EPS-USA program module for reconstructing pressure fields over the continental United States, using the historical pressure measurement database.

(ii) WINDHIST program module for a producing a long term time history of wind speed and direction for any arbitrary location in the contiguous United States.

Applied Research Associates, Inc. Award HI-9361914

Contents

A NEW APPROACH TO ESTIMATE DESIGN WIND CHARACTERISTICS FOR EXTENSIVE PRESSURE SYSTEM STORMS

Andrew Steckley, Peter J. Vickery, Lawrence A. Twisdale Jr.

March 21, 1995

1 INTRODUCTION

The present research investigates a fundamentally new approach for estimating gradient height windspeeds which are driven by extensive pressure systems. First principles are employed to derive windspeeds from the spatial pressure field measured at surface level. This method eliminates many problems associated with the approaches currently used.

The extreme windspeeds in the continental US are produced by a number of meteorological phenomena. In specific regions, however, 50 and 100 year return period windspeeds are generally governed by one or two different phenomena. For example, in the midwestern part of the US, the extreme wind climate is almost exclusively dominated by thunderstorm winds [Twisdale and Vickery, 1993]; the Gulf and Southern Atlantic coastlines are governed by hurricanes; in the northern and northeastern portion of the country, the extreme wind climate is made up of a mixture of winds produced by thunderstorms and extensive pressure systems; and along the Atlantic seaboard, it is a combination of extensive pressure systems and hurricanes. In the winter months, the extreme winds are generally produced by the extensive pressure systems, particularly in the northern and eastern part of the United States.

With the exception of hurricane windspeeds, which are treated using computer simulations, the predictions of extreme windspeeds rely on the direct measurement of windspeeds at the surface (or in some cases upper level windspeed data obtained from balloon measurements). Predictions of windspeeds as a function of return period are then obtained by either fitting the annual extreme to a Fisher-Tippett Type I distribution, or using the hourly windspeed measurements combined with an upcrossing approach. As described in Twisdale and Vickery [1993], the upcrossing approach results in predicted windspeeds that are similar to those derived from non-thunderstorm winds alone. Therefore, the upcrossing approach can only be used in regions where the extensive pressure system (EPS) storms dominate the extreme wind climate.

A limitation common to both the upcrossing approach and the extreme value approach is that both rely on the direct measurement of windspeed at a single site, and these measurements can be influenced bv nearby buildings, vegetation, and local topography. At most stations in the United States, changes in the anemometer height and location have not been fully documented. Also in some cases, the anemometer is located on the roof of a structure and hence it is subject to speed up and shielding effects. In the early 1960's a standard height of 6.1 meters was chosen for the primary reporting stations; however, there are still many stations that do not have anemometers at this level and the quality of the windspeed data is suspect. In all cases, it is assumed that the measuring site is in open country (ANSI Exposure C terrain, with surface roughness length z_0=0.03m). Comparison of the predicted windspeeds at two sites in Chicago [Simui, Changery, and Filliben l979] show differences in the predicted 50 year return period fastest mile windspeeds of 15 mph, even though the two sites are less than 20 miles apart. The present work supports the notion that these differences in predicted windspeeds are caused by differences in anemometer exposure rather than climatic differences. Similar differences are also seen in the comparison windpseeds at the Washington International Airport and the Baltimore Washington International Airport. Simiu et al attribute these results to differences in nearby terrain. Peterka [1992] noted similar differences between predicted windspeeds at nearby stations and attributed these to differences in the upstream terrain at the sites combined with sampling error.

The present research used first principles to derive the windspeeds from the surface pressure field. This method eliminates problems associated with the anemometer heights and exposure. It also reduces the sampling error because in most cases the record length where reliable data is available is longer in the case of pressures than in that of wind speeds. The methodology makes use the National Climatic Data Center's (NCDC) database of recently available digitized measurements from approximately 300 reporting stations throughout the contiguous United States. Hourly records of windspeeds, atmospheric pressure, temperature and several other measurements for these stations are now available on compact disc. Prior to the availability of the CD-ROM data, the approach investigated herein would have been prohibitively expensive. Using the surface

level pressure measurements, the pressure field can be reconstructed enabling estimates of the mean hourly windspeed at gradient height to be determined. This indirect approach is in some ways similar to the approach used to simulate hurricane winds in that the windspeeds are derived from the pressure field, but in the present case the characteristics of the boundary layer flow are better understood and the surface pressure database is far more extensive. The estimation of windspeeds from isobar data has been used in the past; for example, recent work by Maddox and Bezdek [1994] has investigated surface wind-pressure gradient relationships using a small data set. There have been, however, no attempts to use the methodology to determine design windspeeds for land based structures using the full set of available data.

2 DEVELOPMENT OF PRESSURE FIELD APPROACH

2.1 Introduction

In the following sections, the pressure field approach for determining the windspeeds will be developed. The inputs required will be discussed and the scope of the approach with respect to the present investigation will then be defined.

2.2 Basic Equations

The Navier-Stokes equations in an Eulerian reference frame can be expressed

$$\underbrace{\frac{d}{dt}\vec{V}}_{\text{inertial}} + \underbrace{2\vec{\omega}\times\vec{V}}_{\text{Coriolis}} = \underbrace{-s\vec{\nabla}p}_{\text{barospheric}} + \underbrace{s\eta\frac{\partial^2\vec{V}}{\partial z^2}}_{\text{friction}} + \underbrace{\vec{g}}_{\text{gravitational}} \qquad (1)$$

where $\vec{V}$ is the velocity, t is the time, $\vec{\omega}$ is the rotation frequency of the earth, p is atmospheric pressure, s and η are respectively the specific gravity and the coefficient of dynamic viscosity of air, z is the vertical position, and $\vec{g}$ is the gravitational acceleration vector.

Consider the motion at gradient height where by definition the friction term is negligible, and consider only horizontal components for which the gravity term does not contribute. The remaining equation can be then expressed in Cartesian coordinates (x,y) with velocity components (u,v) as

$$\frac{d}{dt}u - \lambda v = -s\frac{\partial p}{\partial x}$$
$$\frac{d}{dt}v - \lambda u = -s\frac{\partial p}{\partial y} \qquad (2)$$

$$\lambda \equiv 2\omega\sin(\varphi) \qquad (3)$$

where λ is the Coriolis parameter, and φ is the latitude.

If one transforms to natural (or tangential) coordinates (s,n) in a Lagrangian frame of reference with components $(V,0)$, then the Navier-Stokes equation may be written as

$$\frac{d}{dt}V = -s\frac{\partial p}{\partial s}$$
$$\frac{V^2}{R} + \lambda V = -s\frac{\partial p}{\partial n} \qquad (4)$$

Here, R is the radius of curvature of the air parcel being considered. The V^2/R term results from the inertial term in the direction of n.

Most considerations of this problem in the engineering literature consider only the steady state case, wherein the pressure field does not vary in time, dV/dt = 0. This reduces Equation 4 to

$$\frac{V^2}{R} + \lambda V = -s\frac{\partial p}{\partial n} \qquad (5)$$

In this scenario, the wind always blows parallel to the isobars and the radius of trajectory curvature is equivalent to the radius of isobar curvature. Neither of these is true in general. In particular, the most extreme winds tend to be associated with large low pressure systems which are moving across the continent. Using the steady state approximation is unsatisfactory in these cases.

There are two difficulties with the practical use of Equation 4. We cannot easily estimate, in a routine manner, either R or dV/dt. In the course of the present research, several techniques for estimating these quantities were investigated in order to implement Equation 4. These included estimating the radius of trajectory curvature by evaluating the radius of isobar curvature and then modifying it to account for the apparent translational speed of the most prominent pressure system. Translational speeds were estimated by tracking low-pressure centers and also by fitting the phase plane of a two-dimensional Fourier transform of the pressure field. These techniques proved to be good for specific cases but not for general application. As a result, it was decided to return to the fundamental equations of motion in the Eulerian reference frame.

In the following sections two successive approximations of the gradient level windspeed have been derived directly without transformation to a Lagrangian reference frame. This approach of successive approximations was suggested by Van Meigham [1941].

2.2.1 First Approximation

Return to Equation 2 and solve for u and v. For convenience and brevity, adopt the notation of subscripts for partial differentiation (i.e. $dp/d_X = p_x$, etc.) and define the inverse of the Coriolis parameter as

$$a \equiv \lambda^{-1} \tag{6}$$

We then have

$$\begin{aligned} u &= -sap_y - a\frac{d}{dt}v \\ v &= +sap_x + a\frac{d}{dt}u \end{aligned} \tag{7}$$

Now as a first approximation, assume that

$$\frac{d}{dt}\vec{V} = 0 \tag{8}$$

Implementing this assumption in Equation 7 produces the *geostrophic wind, V^g,* with components u^g and v^g defined as

$$\begin{aligned} u^g &\equiv -sap_y \\ v^g &\equiv +sap_x \end{aligned} \tag{9}$$

2.2.2 Second Approximation

As a second approximation, assume

$$\frac{d}{dt}\vec{V} = \frac{d}{dt}\vec{V}^g \tag{10}$$

or

$$\begin{aligned} \frac{d}{dt}u &= \frac{d}{dt}u^g \\ \frac{d}{dt}v &= \frac{d}{dt}v^g \end{aligned} \tag{11}$$

Implementing this assumption in Equation 7 produces

$$\begin{aligned} u^{<2>} &= -sap_y - a\frac{d}{dt}(sap_x) \\ v^{<2>} &= +sap_x - a\frac{d}{dt}(sap_y) \end{aligned} \tag{12}$$

or

$$\begin{aligned} u^{<2>} &= -sap_y - a^2 p_x \frac{d}{dt}s - sap_x \frac{d}{dt}a - sa^2 \frac{d}{dt}p_x \\ v^{<2>} &= +sap_x - a^2 p_y \frac{d}{dt}s - sap_y \frac{d}{dt}a - sa^2 \frac{d}{dt}p_y \end{aligned} \tag{13}$$

Recall that in the Eulerian reference frame, we require the total derivative with respect to time. That is, $d/dt \neq \partial/\partial t$, but rather, $d/dt = \partial/\partial t + u\partial/\partial x + v\partial/\partial y$. Consistent with our previous assumption, we will approximate this derivative by using u_g and v_g in place of u and v. At this point we will define positive x and y directions as east and north respectively. We then have

$$\frac{d}{dt}s = s_t - sap_y s_x + sap_x s_y \tag{14}$$

$$\frac{d}{dt}a = sap_x a_y \tag{15}$$

$$\frac{d}{dt}p_x = p_{xt} - sap_{xx}p_y + sap_{xy}p_x \tag{16}$$

$$\frac{d}{dt}p_y = p_{yt} - sap_{xy}p_y + sap_{xx}p_x \tag{17}$$

In Equation 15, we have recognized that the inverse Coriolis parameter is invariant in the east-west (x) direction and in time. Substituting these expressions into Equation 13 gives

$$\begin{aligned} u^{<2>} &= -sap_y - a^2 p_x s_t + sa^3 p_x (p_y s_x - p_x s_y) \\ &\quad -s^2 a^2 p_x^2 a_y - sa^2 p_{xt} + s^2 a^3 (p_{xx}p_y - p_{xy}p_x) \\ v^{<2>} &= +sap_x - a^2 p_y s_t + sa^3 p_y (p_y s_x - p_x s_y) \\ &\quad -s^2 a^2 p_x p_y a_y - sa^2 p_{yt} + s^2 a^3 (p_{xy}p_y - p_{yy}p_x) \end{aligned} \tag{18}$$

Fortunately not all of these terms will be significant. The following table shows indicative values for each of the variables involved in the above equation. Those which are dependent on latitude are shown for a range from approximately 20° to 50° North latitude.

The pressure derivative values shown are 99th percentile values determined from actual data.

Variable	Indicative Value (typical or extreme)	
s	1	m^3/kg
s_x, s_y	$5\text{x}10^{-7}$	m^2/kg
s_t	$3\text{x}10^{-6}$	$m^3/kg/s$
a	20000 - 9000	s
a_y	0.001 - 0.007	s/m
p_x, p_y	0.003	Pa
p_{xt}, p_{yt}	$2.7\text{x}10^{-7}$	Pa/s
p_{xx}, p_{yy}	$8\text{x}10^{-11}$	Pa/m

Using these values, we can estimate the relative importance of each term. To do this, values of s, s_x, s_y, and s_t from the previous table have been used along with a large sample of actual pressure gradient data. For each sample, the ratio of magnitudes of each term to the total of all terms has been calculated.

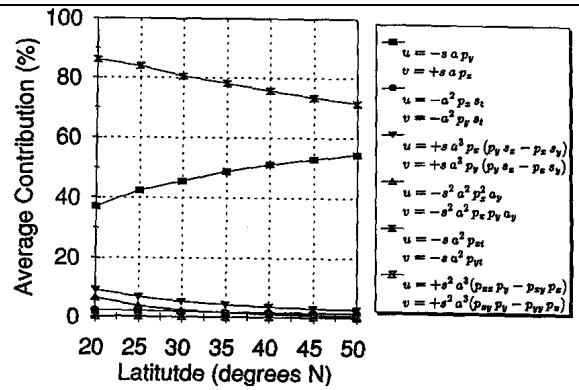

Figure 1: Relative Contribution of Terms

The average values of these ratios are shown in Figure 1 for a range of latitudes covering the contiguous United States. This approach provides only a rough indication of the relative magnitudes of the terms, which may occur. In most cases, the extreme values will not occur coincidentally and there are likely to be terms of opposite signs, which cancel out most of the contributions. These calculations should only be interpreted as an approximate indication of which terms could potentially contribute to the overall estimate.

We can now rearrange Equation 18 ordering the terms according to their expected importance.

$$
\begin{aligned}
u^{<2>} = & -sap_y \\
& -sa^2 p_{xt} \\
& -s^2 a^2 p_x^2 a_y \\
& +sa^3 p_x (p_y s_x - p_x s_y) \\
& +s^2 a^3 (p_{xx} p_y - p_{xy} p_x) \\
& -a^2 p_x s_t \\
v^{<2>} = & +sap_x \\
& -sa^2 p_{yt} \\
& -s^2 a^2 p_x p_y a_y \\
& +sa^3 p_y (p_y s_x - p_x s_y) \\
& +s^2 a^3 (p_{xy} p_y - p_{yy} p_x) \\
& -a^2 p_y s_t
\end{aligned}
\qquad (18)
$$

Note that the first term alone is equivalent to the first approximation or the geostrophic wind. The second term considers the time rate of change of the pressure field and adds a velocity component, which is aligned with the isallobars of the pressure field. It is therefore referred to as the isallobaric component.

A few points are worth noting from Figure 1. The geostrophic and isallobaric terms are the most significant and can potentially be of the same order. The remaining terms may potentially be significant but are secondary. The terms containing p_{xx} and p_{yy} are essentially negligible.

2.3 Input Parameters Required

Equation 18 relies on three sets of input parameters. These are discussed separately in the following sections.

2.3.1 Pressure Field Gradients

These consist of the spatial and temporal derivatives of the pressure field. Specifically, p_x, p_y, p_{xx}, p_{yy}, p_{xy}, p_{xt}, and p_{yt}, evaluated at the gradient windspeed height where the assumption of purely horizontal motion is most valid. In principle, we can estimate all of these quantities by modeling the sea level pressure field from station measurements and then evaluating the required derivatives. The assumption is that these derivatives are equivalent to those at the gradient windspeed height.

2.3.2 Inverse Coriolis Parameter and Gradient

The quantities, a and a_y, are easily determined for any specific location of interest. They are

$$a = \frac{1}{2\omega \sin(\varphi)} \tag{19}$$

$$a_y = \frac{-\cos(\varphi)}{2R_g \omega \sin^2(\varphi)} \tag{20}$$

where φ is the latitude and $R_g \approx 6.5x10^6 m$ is the distance from the center of the earth to gradient windspeed height.

2.3.3 Specific Volume and Gradients

The specific volume (or inverse density) of the atmosphere and its spatial and temporal derivatives are also required. These are the quantities, s, s_x, s_y, and s_t. They may be estimated by first determining the temperature and pressure at the location of interest and assuming the ideal gas law is applicable. The NCDC database from which the pressure measurements are available also includes hourly readings of temperature. To the extent that one can interpolate the temperature (and pressure) at the geographic location of interest and then extrapolate to the gradient windspeed height, one can determine reasonable estimates of the specific volume and its gradients. This is an area for further research.

2.4 Scope of the Approach for the Present Study

It was not feasible to consider all of the terms in Equation 18 within the scope of this research. Since our present purpose was to establish feasibility of the overall approach, we have considered only the two most significant terms - the geostrophic and the isallobaric.

Accordingly, two separate windspeed estimates are evaluated in the present study. They are:
Geostrophic:

$$u = -sap_y \qquad v = +sap_x \tag{21}$$

Isallobaric:

$$u = -sap_y - sa^2 p_{xt} \qquad v = +sap_x - sa^2 p_{yt} \tag{22}$$

Although the second model contains both terms, it is referred to here as the isallobaric approximation for convenience. These estimates require only the modeling of the first derivatives of the pressure field and evaluation of the specific volume and Coriolis parameter The additional terms would require estimating the spatial curvatures of the pressure fields as well as the temporal and spatial derivatives of specific volume and Coriolis parameter. The additional effort required for these less significant terms was considered inappropriate in this phase of the research. Also a steady value of specific volume has been used for all calculations.

In later sections of this report, comparisons are made with actual surface windspeed measurements. Some investigation has been carried out to ascertain the effect of the neglected terms and the use of a steady value of specific volume.

3 PRESSURE FIELD RECONSTRUCTION

The windspeed estimates outlined in the previous section require the evaluation of pressure gradients at any geographic location of interest. Consequently, the first task of the present research was to develop and evaluate an approach for reconstructing the pressure field over the United States using available point station readings. The Surface Airways database of the National Climatic Data Center was used. This database is available on CD-ROM from Earthlnfo Inc. of Boulder Colorado. It contains hourly readings of atmospheric pressure corrected to sea level for approximately 300 weather stations located throughout the contiguous United States for the period from the late 1940's to present. There are some practical problems with the completeness of the database both spatially and temporally; these will be discussed in a following section. First, the interpolation method used to reconstruct the pressure field for any given hour will be discussed.

3.1 Contour Mapping from Scattered Stations

The purpose of producing contour maps is to demonstrate and confirm that we can routinely reduce the historical pressure data from a set of scattered stations to a continuous pressure field or contour map, and that the results do not contradict, in any significant way, the pressure contour maps produced by other researchers. In particular, in order to process long term time histories of pressures gradients, it was necessary to develop a method which could be reliably automated in computer software.

There are two aspects of the contour mapping that differ in their importance to the present task: proper local interpolation and gross feature presentation. The purpose of most available pressure contour maps is for identification and presentation of gross weather system features (cold fronts, low pressure systems, etc.). There are numerous software packages available which produce presentable contour maps from discrete scattered data points. Many such packages use standard triangularization techniques to

establish a regular grid of discrete data points, and then use simple linear interpolations to graphically draw consistent contour lines. These maps are "correct", in that they do not contradict the discrete data, appear to be physically plausible realizations of the pressure field, and compare adequately in their gross features with other contour maps such as those produced by NCDC. They can, however, be entirely inadequate when it comes to our primary task of interpolating the correct pressure gradients at specific point locations in order to perform detailed calculations.

With this in mind, our focus has been on producing a reliable, physically rooted, approach to interpolating the pressure field at any specific point in the domain. The subsequent presentation of contour maps then amounts to using this approach to produce as fine a regular grid of discrete points as necessary to produce a presentable contour map; any inadequacy of the interpolation techniques used in a particular drawing routine can be cured by producing a finer grid.

It is important to realize here that a good comparison between contour maps does not necessarily imply that that appropriate interpolations have been made at specific points. In fact, rougher grids of data will generally agree better with weather maps produced by hand interpolations.

There are a number of methods for interpolating from scattered data. This problem can be broken into two parts; subset selection and interpolation method.

3.1.1 Subset Selection

There are essentially three approaches to selecting a subset of available discrete stations to use for interpolating at a specific point: fixed number (using the n nearest neighbors), fixed distance (using all stations within a chosen distance d), or natural neighbor subsets. Natural neighbors are defined using an empty circumcircle criterion. The natural neighbors of a point A, are the set of stations from which the circumcircle of any two along with the point A does not contain any other station. Natural neighbors are less simple to select but are more appropriate for scattered data in which the density of stations varies. The number of natural neighbors for different points in a domain varies but is rarely greater than 13.

For subset selection in the present work, the following procedure was used. First the set of stations having valid data on the date and hour of interest is determined as the base set. Then the nearest station to the interpolation point is located. Next all of the natural neighbors of this stations and all of *their* natural neighbors are selected. This procedure applied to the set of available weather stations produces a subset typically numbering 30 - 40. (Whenever the number of selected stations exceeds 85, however, the nearest 85 stations are chosen instead. This was necessary to accommodate computer memory limitations which arise later in using the subset for interpolating.)

3.1.2 Interpolation Method

There are two basic approaches to interpolating: fitted functions and weighted averages. In this work, weighted averages were ruled out because it was desired that each of the recorded data points fall directly on the interpolated surface. In doing this, it is assumed that the historical pressure measurements are both precise and accurate. These assumptions are discussed further in the next section.

A planar plus minimum curvature spline fitting approach was selected. The spline approach distributes the changes in slope as widely and evenly as possible. The resulting surface has the least possible change in slope at all points and is obtained by minimizing the total curvature. In effect, this assumes that the pressure field over the United States is a constant plane except insofar as it *needs* to be distorted in order to match the known pressures at certain locations. While the "true" pressure field may have higher gradients than that indicated by fitting the known data points with a surface of minimum curvature, it seems inappropriate to introduce higher gradients without justifications from the known data.

For N stations located at (x_j, y_j) with pressure measurements P_j, N+3 simultaneous equations are solved:

$$P_j = b_0 + b_1 x_j + b_2 y_j + \sum_{i=1}^{N} C_{ij} a_i \quad ; \quad j = 1,...,N \tag{23}$$

$$\sum_{i=1}^{N} a_i = 0 \quad ; \quad \sum_{i=1}^{N} a_i x_i = 0 \quad ; \quad \sum_{i=1}^{N} a_i y_i = 0 \tag{24}$$

where

$$C_{ij} = ((x_i - x_j)^2 + (y_i - y_j)^2)\log[(x_i - x_j)^2 + (y_i - y_j)^2] \tag{25}$$

resulting in the N+3 coefficients, a_i, b_0, b_1, b_2. The value at any point in the domain may then be interpolated by

$$P(x,y) = b_0 + b_1 x + b_2 y + a_i C_i(x,y) \tag{26}$$

where

$$C_i(x,y) = ((x_i - x)^2 + (y_i - y)^2)\log[(x_i - x)^2 + (y_i - y)^2] \quad (27)$$

Nuss and Titley [1994] recently investigated the use of multi-quadric interpolations for reconstructing pressure fields. Thier method is very similar to that used in the present work, except that the basis functions defined by Equations 25 and 27 were different. They used

$$C_{ij} = -(\frac{(x_i - x_j)^2(y_i - y_j)^2}{c^2} + 1.0)^{1/2} \quad (28)$$

$$C_i(x,y) = -(\frac{(x_i - x)^2(y_i - y)^2}{c^2} + 1.0)^{1/2} \quad (29)$$

where c is an arbitrary and typically small constant. They first removed the average of the data and did not include fitting the planar trend. In effect this means they included b_0 but considered b_1=b_2=0;

3.2 Assessment of the NCDC Database and the Interpolation Approach

As discussed in the introduction, air pressure measurements are generally more robust than anemometer measurements and suffer fewer problems associated with instrument maintenance, placement, sheltering and averaging time effects; this is in part the impetus for the development of the present approach. Nevertheless, there are some problems with the available database which need to be addressed.

Although the NCDC database covers an extensive period - in excess of 40 years - and contains excellent spatial coverage for the vast majority of the contiguous United States, it is unfortunately far from complete. Not all stations were operating through the entire period. In addition, some stations adopted different recording practices for certain periods. For example, some stations do not have readings through the night time hours, presumably due to unavailability of staff. During the late 1960's and early 1970's many stations took readings every third hour rather than hourly.

In no cases does this result in too little data to perform the necessary interpolations. It does however result in a non-uniformity that complicates the process of evaluating long term time histories of pressure gradients and subsequently windspeeds. For each hour to be evaluated, the database must be examined to determine which stations have valid data available, and the appropriate subset of stations to use in interpolating must be re-evaluated.

A second difficulty arises in part due to the choice of interpolation method. Both the minimum curvature spline approach and the similar multi-quadric approach used by Nuss and Titley [1994] apply to data whose observation errors can be considered negligible. The fitted surfaces are forced to pass through each measured data value. This causes a problem particularly in regions where two or more weather stations are very closely located. Although the pressure measurements may be in essential agreement, interpolated pressure *gradients* in the vicinity will be overly sensitive to small random measurement errors. Of course, the interpolations are also sensitive to any single inaccurate measurement even though it may be only one of several dozen used in the interpolation.

Many common alternative methods, such as kriging, do not have this problem because, in general, they do not force the surface through every measured data point. Kriging also has the advantage that the interpolating coefficients (after having been established on the basis of the spatial correlation structure of the total data set) depend only on the geometry of the location of interest relative to the station subset and not on individual data measurements. This means that for a given location and subset, the coefficients need to be evaluated only once. Then only the interpolating equation needs to be used for each set of measurements. This results In significantly less computing time to produce a long term time history.

While these advantages of kriging are acknowledged, it is felt that the minimum curvature spline approach should be maintained. This latter approach was chosen for a couple of subtle but important reasons. First, it was appealing with respect to the physical notion of distorting the pressure field from a plane (and hence introducing pressure gradient) only as much as required to fit the known data. Second, it maintains a "local" focus on the data in both space and time, because it uses station specific and time-coincident data in its interpolations. This is important when one is trying to estimate higher order local features such as gradients. Kriging, on the other hand, relies on the total statistics of the data in either space and time or both (depending on how one applies it) and in so doing, compromises the "local" focus. Also supporting the choice of minimum curvature splines is the fact that the work of Nuss and Titley used a very similar technique and they confirmed that it was superior to most alternatives when one is interested in capturing local features of the pressure field.

Most difficulties associated with the database can be alleviated by performing a comprehensive data patching and "reconditioning" procedure. It is suggested that the database first be analyzed to identify and remove those measurement data, which are clearly inaccurate or inconsistent with nearby measurements in both space and time. Then the entire database should be processed to fill in all missing values by appropriately interpolating in both space and time. Stations with unacceptably high amounts of interpolated data could be removed from the base set. Additionally, the base set could be reduced by removing stations, which are within a minimum distance of other stations, or averaging these stations together to form single virtual stations.

A complete review and repair of the database will be conducted in Phase II of the research.

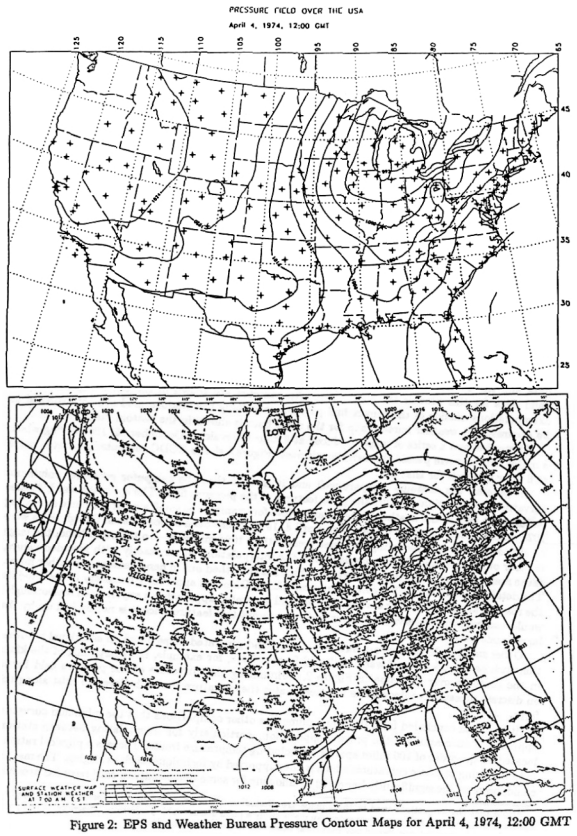

Figure 2: EPS and Weather Bureau Pressure Contour Maps for April 4, 1974, 12:00 GMT

Figure 2. EPS and Weather Bureau Pressure Contour Maps for April 4, 1974, 12:00 GMT

3.3 Comparisons of Contour Maps

Numerous pressure contour maps were produced by computer using the above approach and compared to hand generated weather maps from other sources. One such comparison is shown in Figure 2. The top map shows the 4 millibar pressure contours derived using all available pressure data and the automated minimum curvature spline approach. The weather stations contributing valid data for this process are also shown. No contours are shown in the outer regions because extrapolations outside of the convex hull polygon containing the stations used are not expected to be accurate. A weather bureau map for the same hour is shown in the bottom map[1].Figure 3 shows a series of maps produced at 3-hour intervals for December 15, 1987 during which a major winter storm passed through the Midwest. Figure 4 shows NCDC computer generated maps at 6 hour intervals for that day.

In general, the contours compare well and it is clear that the computer generated minimum curvature interpolations capture the gross features of the pressure field. The approach also indicates features not seen in the weather bureau maps. Note for example the small area of pressures exceeding 1024 millibars over northern Colorado on April 4, 1974 (Figure 2). It has been indicated even though there were no stations in the area recording pressures greater than 1024 millibars. On the other hand, the large number of stations and the requirement that the interpolations agree exactly with recorded values, cause many smaller scale features to result which are smoothed out in hand generated weather maps. The detail in the 1004 millibar contour around Akron, Ohio was apparently necessary to accommodate the reading at that particular station. In the hand generated approach, an experienced meteorologist would assume some observational error and smooth out this feature since it is not backed up by the larger scale pattern.

Other small-scale features are included in the hand generated maps based on additional information such as the presence of warm and cold fronts. Note, for example, the sharpening of the kinks in the contours over Alabama in Figure 2. Minimizing the curvature of the pressure field based on discrete pressure readings alone underestimates the curvature that is believed to exist along the front.

It has been concluded from these and numerous other comparisons that the minimum curvature approach is successful for the present application, particularly for interpolating between stations located on the order of 100 miles apart and excluding temperature fronts. There is a physical rationale for minimizing pressure curvatures, which is not supported by techniques such as kriging. The method could, however, be

[1] Note that the projections used in these maps are dissimilar; those produced by the present software apply an Albers conic projection while the weather bureau maps apply a polar stereographic projection. Therefore, in comparing particular contour paths, one should pay particular attention to geographic landmarks.

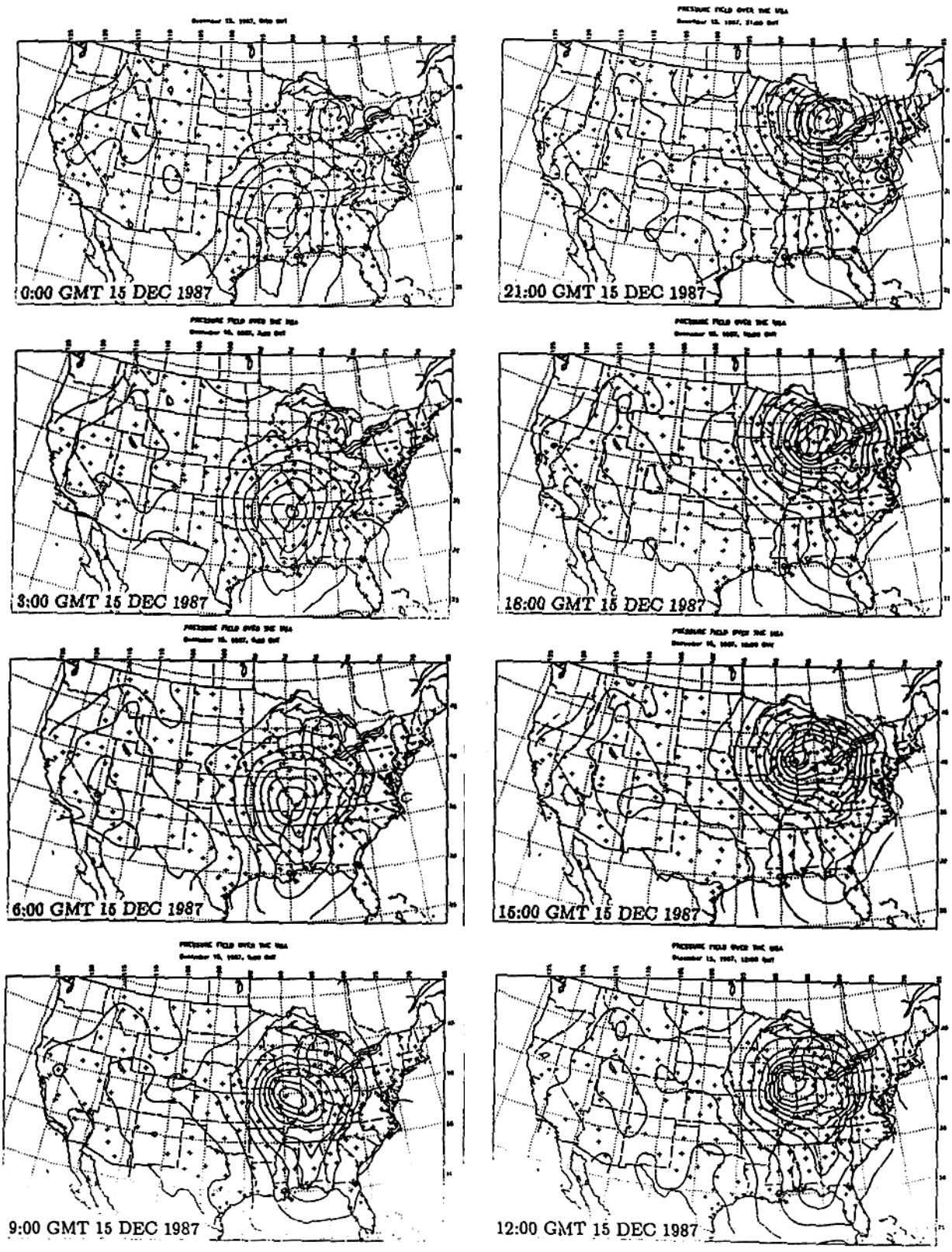

Figure 3. EPS Pressure Contour Maps at 3 Hour Intervals on December 15, 1987

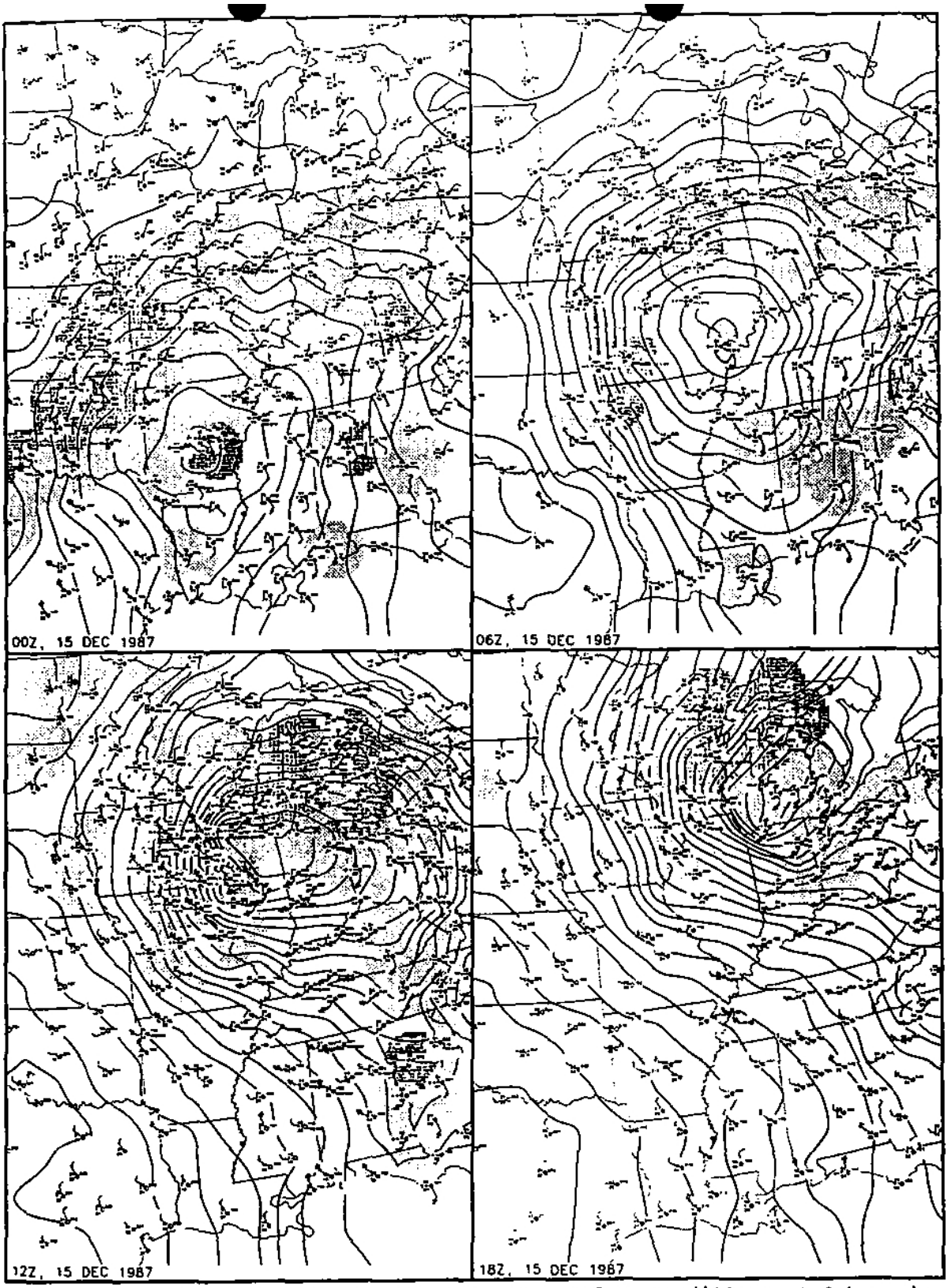

Computerized data plot and analysis maps show surface conditions at 6-hour intervals during the storm's intensification phase on December 15th (UTC). Isobars are at 2 mb intervals. ---Maps by Brian E. Doty, University of Maryland.

Figure 4. NCDC Pressure Contour Maps at 6 Hour Intervals on December 15, 1987

improved by allowing for some uncertainty in each recorded pressure.

Without this relaxation, it may produce wildly inaccurate pressure gradients near stations, which are closely located.

Based on the map comparison results, the present minimum curvature interpolation approach -- assuming no observational error --- was considered acceptable for the purpose of establishing feasibility of the pressure field approach. It is recommended that the suggested improvements be developed in Phase 2 research.

4 SURFACE LEVEL WINDSPEED TIME HISTORIES

4.1 Relations Between Gradient and Surface Winds

The roughness of the earth's surface introduces shearing forces within the atmospheric boundary layer. These forces, indicated by the friction term in the basic Navier-Stokes equation shown in Section 2.2, affect both the speed and the direction of the wind. As one descends from gradient height, the windspeed decreases to meet the boundary condition of zero velocity at the surface. This decrease in speed reduces the Coriolis forces proportionally, and in order to maintain a balance of horizontal momentum, the wind vector rotates. This "Ekman" spiral results in a counter-clockwise rotation of the velocity vector with decreasing height in the northern hemisphere and a clockwise rotation in the southern hemisphere. Values in the range from 0° to 45° are typically observed.

The vertical profile of mean hourly windspeed is best modeled in the lowest regions below about 50 m by a log-law model. A power-law model is often used to match the profile above this. Cook [1985] presents an empirical model developed by Deaves and Harris [1980] which matches the profile well throughout the Ekman layer. Their equation for equilibrium mean wind profile is

$$V = 2.5u_*\{\ln[\frac{z}{z_0}] + 5.75(\frac{z}{z_g}) - 1.875(\frac{z}{z_g})^2 - 1.333(\frac{z}{z_g})^3 + 0.250(\frac{z}{z_g})^4 \qquad (30)$$

where u_* is the friction velocity, z_0 is a characteristic roughness length, and z_g is a gradient reference height. Typical values for an open country exposure are $u_* \approx 0.0689 V_{10} m/s$, $z_0 \approx 0.03m$, and $z_g \approx 2550m$, and V_{10} is the mean velocity at 10 *m* above ground. This suggests a ratio between the windspeed at gradient height and at 10 *m* of 2.43.

An open country exposure is most often assumed when using weather bureau data; however, the actual exposure at the anemometer site may well vary due to upstream terrain as well as local speed-up and sheltering around the anemometer. The choice of exposure and the corresponding parameters to describe it is a source of practical uncertainty in modeling wind climates and relating upper level wind speeds to those at or near the surface. In previous research by the first author, a site that was deemed by several experienced wind engineers and meteorologists to be isotropic in exposure type was later found through field measurements to have a characteristic surface roughness z_0 which varied by a full order of magnitude around the azimuth. This can translate into a 10% or 15% variation in the ratio of windspeeds at 10m to those estimated at gradient height.

Conventional approaches for determining design windspeeds at a site typically require subjective assessments of exposure conditions at multiple locations. First the exposure conditions at the recording site are required in order to relate the surface windspeed measurements to a reference height; most often an open country exposure is assumed without further verification. The reference winds are then related to surface winds at a design site through an assessment of exposure conditions there, usually by designers guided by code procedures. There is plenty of room for the introduction of uncertainty in this overall process. The approach being investigated in the present research does not escape this problem entirely, but by assessing gradient level windspeeds directly from the pressure field, one major element of subjective exposure assessment is removed.

4.2 Comparisons of Selected Time Histories from 1987

As an initial assessment of the pressure field approach, comparisons of both geostrophic and isallobaric approximations were made with windspeeds measured by surface anemometers at four locations. Comparing these data is a difficult task and requires several assumptions and adjustments. Without a detailed time history of upper level winds on an hour by hour basis, however, this represents the best direct comparison one can make.

Four locations were chosen for comparison: Minneapolis, MN; Chicago, IL; Dayton, OH; and Dallas, TX. At each of these locations, one-minute average windspeeds have been recorded hourly at the local airports. The anemometers are located at various heights from 6-10 m. The open country profile defined by Equation 30 was assumed. All

surface level windspeeds as well as the gradient height windspeeds derived from the reconstructed pressure fields were converted to a height of 10 m. A counter-clockwise Ekman rotation of 45° in wind direction was assumed between gradient height winds and those at 10 m.

Figures 5 to 8 show time histories at each location for the period February 1-10, 1987. The upper plot in each figure shows windspeed and the lower plot shows wind direction. The surface windspeed measurements, along with both the geostrophic and isallobaric estimates are given in each plot.

Higher frequency variations are noticeable in the surface time histories. This is due in part to the fact that the surface measurements are only one minute averages and thus include some of the turbulent wind energy present in the lower boundary layer. (The resolution of each measurement is also limited to 0.515 *m/s* as each is recorded in whole knots.) In addition, before deriving the geostrophic and isallobaric estimates, the pressure gradient time histories were low-pass filtered at a cutoff frequency corresponding to 4 hours, thereby providing some temporal smoothing. (The modifications to the NCDC database recommended in Section 3.2 would provide complementary spatial smoothing.)

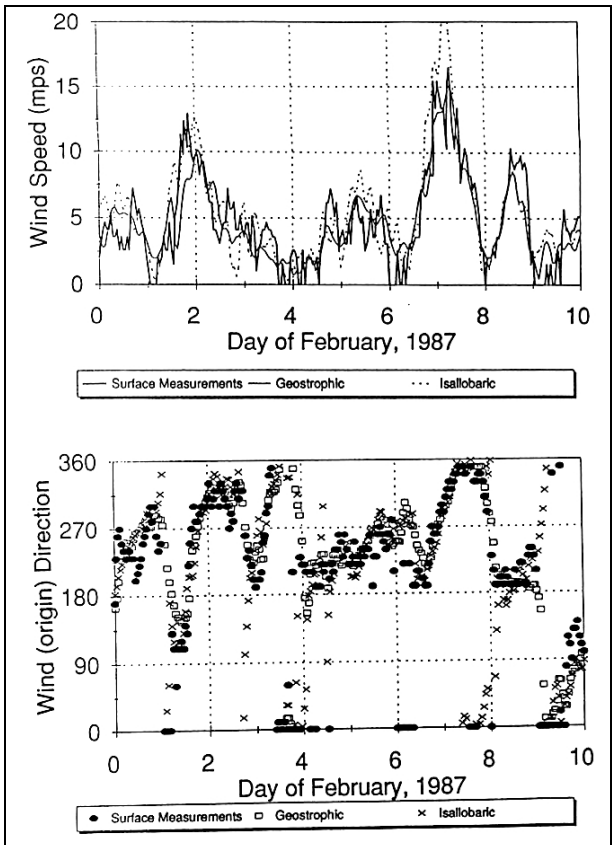

Figure 5. Surface Level Wind Comparisons for Minneapolis

4.3 Discussion of Results

Considering the uncertainties involved regarding upwind exposure and hence also the conversions from gradient wind vectors to those at 10m, the comparisons are remarkably good. The major variations in both speed and direction are clearly captured by even the geostrophic estimate. In order to fully assess these comparisons, a more detailed statistical analysis of deviations between measured and derived wind vectors was carried out and these are described in the following section.

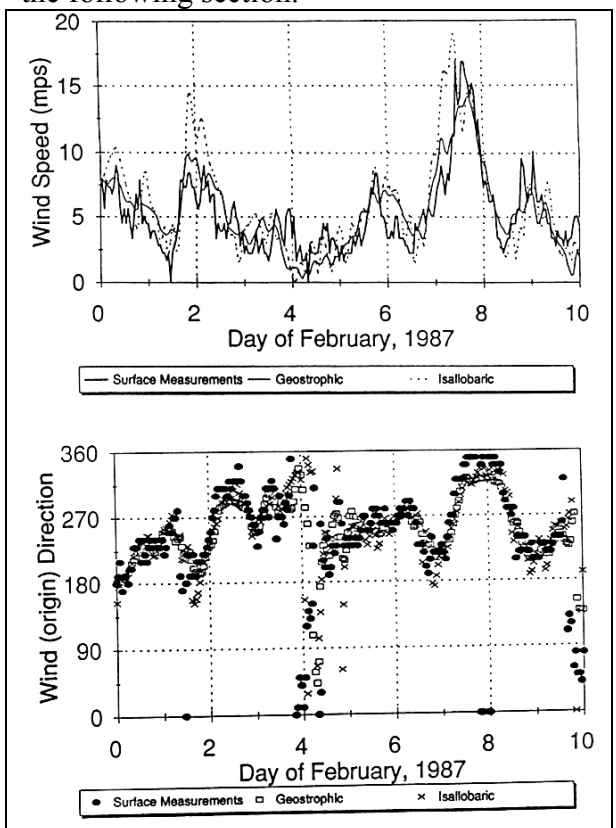

Figure 6. Surface Level Wind Comparisons for Chicago

4.3.1 Statistical Analysis of Differences with Measured Data

Detailed analysis of the hour-by-hour time series were performed on the results for windspeeds at Minneapolis, Chicago, and Dayton. Long term time histories of both measured and derived wind vectors for the period from 1964 to 1991 were compared to determine how the deviations varied with measured windspeed magnitude and direction, and with hour of

the day. The relative difference in windspeed has been defined as

$$\varepsilon_s = \frac{d_s - m_s}{m_s} \tag{31}$$

where m_s is the measured wind speed and d_s is the derived windspeed computed using either the geostrophic or isallobaric approximations. The difference in wind direction is simply that between the measured and derived values *before* any estimated allowance for the Ekman rotation. In the interests of space only representative plots have been included here, but the conclusions drawn are supported by all of the results.

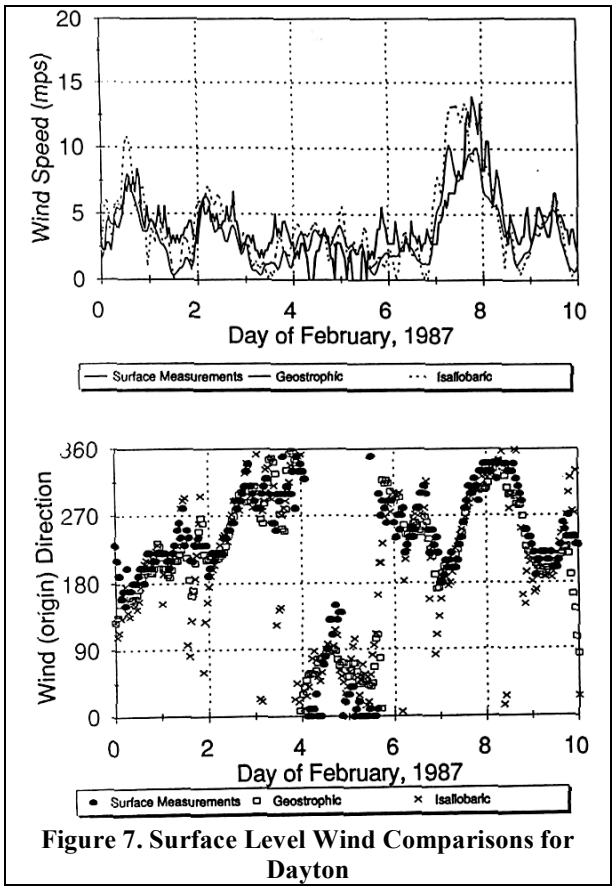

Figure 7. Surface Level Wind Comparisons for Dayton

Variations with Windspeed

Figures 9 and 10 show the variation of the mean relative difference between the derived and the measured wind vectors for Minneapolis and Chicago. Statistically, the derived windspeeds are in much better agreement at higher windspeeds. This is not unexpected; at lower windspeeds, there will be many more situations of atmospheric instabilities, which are not considered in the assumed wind profile, nor in the derived approximations used. There will also be greater resolution error in the measured data. In general, however, the stronger windspeeds will be associated with synoptic scale forcing mechanisms, which are inherent in the pressure field approach. The differences with measured data seen at low windspeeds are not significant since the approach developed herein is directed towards estimating high windspeed occurrences only.

The isallobaric estimates show better statistical agreement at the higher windspeeds; however, two points should be noted. First, the surface measurements may also contain winds from non-synoptic scale mechanisms such as thunderstorms, which are not included in the pressure field approach. This may cause a minor bias toward underestimation. Second, the derived windspeeds are directly proportional to the assumed value of specific gravity of the atmosphere, i.e. inversely proportional to air density. An air density value of 1 kg/m^3 was used without variation in either time or space. This is expected to be a representative value for the atmosphere at gradient height; however, it will undoubtedly vary particularly with temperature and pressure. As a consequence, diurnal variation in air density can be expected and no allowance for this has been considered in the present results. The variation of mean difference in wind direction, seen in the lower plots, shows a distinct trend with measured

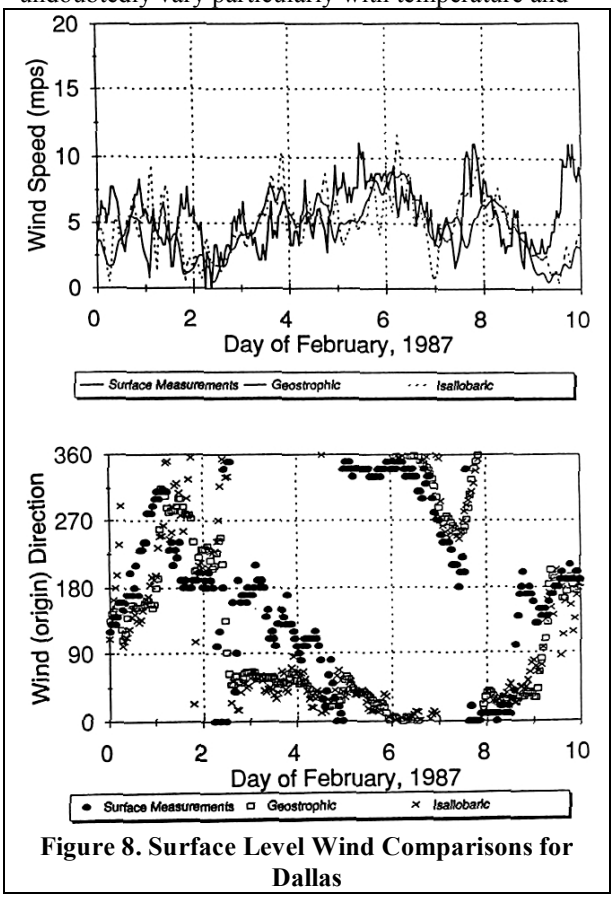

Figure 8. Surface Level Wind Comparisons for Dallas

windspeed as well, since the amount of Eckman rotation is a function of the windspeed.

Variations with Wind Direction

Based on the above findings, the statistical analysis of variations with wind direction was performed only on data for which the measured windspeed exceeded 5 *m/s*. Figures 11 and 12 show the variation of differences for Dayton and Chicago. As expected there is a particularly strong trend with wind direction and the details differ from city to city. These results underscore the uncertainties associated with anemometer exposures, both in the previous comparisons of time histories and in the conventional approach for determining wind climate models from surface anemometer data. Remember that these plots show the mean difference from a more or less continuous time history of 27 years. Hence, most other direction independent sources of error and variation have been averaged out, (even those having annual or seasonal variations.) For Chicago, the upwind exposure assumptions alone can account for overestimates on the order of 30-40% for some directions and underestimates of 20% for others.

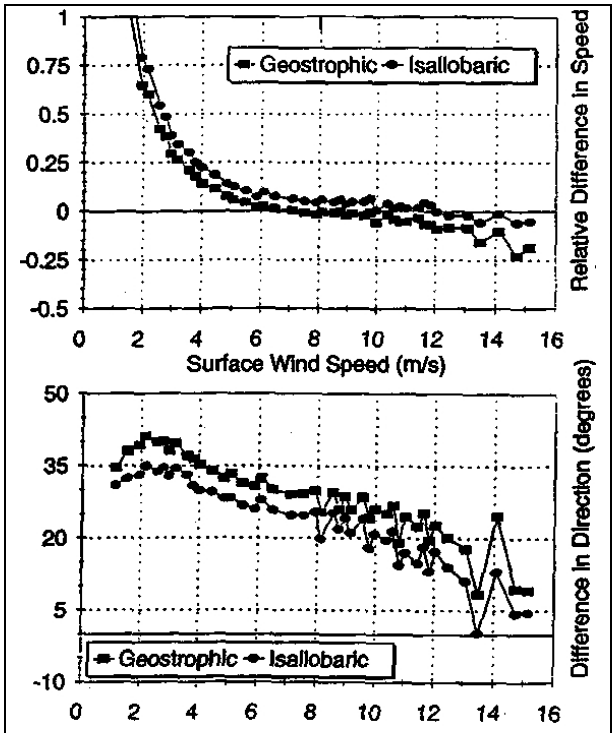

Figure 9. Variation of Differences with Windspeed for Minneapolis

Variations with Time of Day

Figures 13 and 14 show the variation of differences with the hour of the day for Minneapolis and Dayton. This has been examined as an indirect measure of the effects of air density variation. Again, the only data included is that for which the measured windspeed exceeded 5m/s (where previous results suggest that the differences between calculated and measured values are relatively independent of windspeed.) Again there is a very strong trend shown in the windspeed and it is on the order of variation expected in the diurnal cycle of air density. During the daytime hours, the differences are smaller suggesting that a higher value of specific volume than that used is required. This is consistent with the expectation of a lower air density during the warmer daytime hours.

One would expect the differences between calculated and measured values of wind direction to be a function of hour only insofar as the wind climate may have a directional correlation with time of day and through the coupling of windspeed and direction effects seen in the previous results. This is also consistent with the present results.

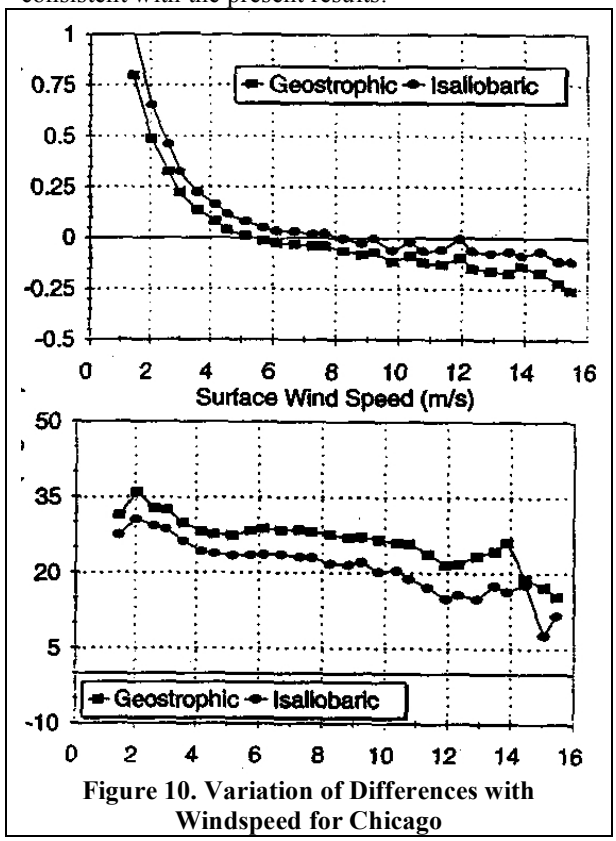

Figure 10. Variation of Differences with Windspeed for Chicago

4.4 Detailed Analysis of Crossing Rates for Minneapolis

Crossing rate functions were calculated for each of the available time histories and comparisons were made between measured and derived sources. Crossing rate functions are discussed further in Section 5.1.3 where an expression for efficient calculation from discrete time histories is given. Figure 15 shows the comparison of crossing rates for Minneapolis.

In this case, the measured surface windspeeds have been converted to gradient height using the profile of Equation 30 to correspond to the derived estimates.

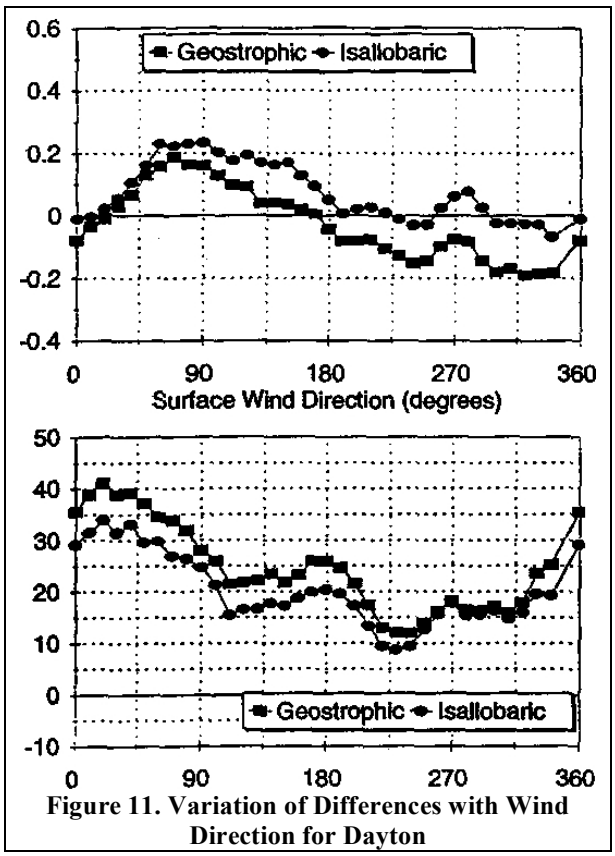

Figure 11. Variation of Differences with Wind Direction for Dayton

About 96% of the measured windspeeds correspond to the range below 50 mph and in this range the crossing rate from the isallobaric approximation is in excellent agreement with the crossing rate from the measured data. Above this range, however, the crossing rate is significantly overestimated.

Some overestimating was expected based on a visual inspection of the time histories, however, it was not clear that it would be as large as the amount seen in these calculations. The crossing rate of the 100 *mph* level for example is about 10/*yr* whereas the measured data suggest a value on the order of 0.2/*year* (or a return period of about 5 years).

It is possible that the random errors inherent in the derived processes were such that they caused multiple local peaks during times in which the measured windspeeds presented only a single peak. In order to determine if such artificial clustering of peaks was occurring, duration functions were estimated for the case of Minneapolis. These are shown in Figure 16. These are defined as the ratio of cumulative distributions to crossing rates as follows:

$$D^{+}(v) = \frac{\int_{v}^{\infty} p_v(v)dV}{N(v)} \tag{32}$$

$$D^{-}(v) = \frac{\int_{-\infty}^{v} p_v(v)dV}{N(v)} \tag{33}$$

where $p_v(v)$ is the probability density function of the process and $N(v)$ is the crossing rate function. The D^+ functions decrease with increasing speed while the D^- functions increase. For a given process, these two functions equal each other at the mean value. For values of v much higher than the mean, D^+ provides a measure of the average duration of an exceedance of the level v while D^- effectively provides a measure of the average time between such exceedances.

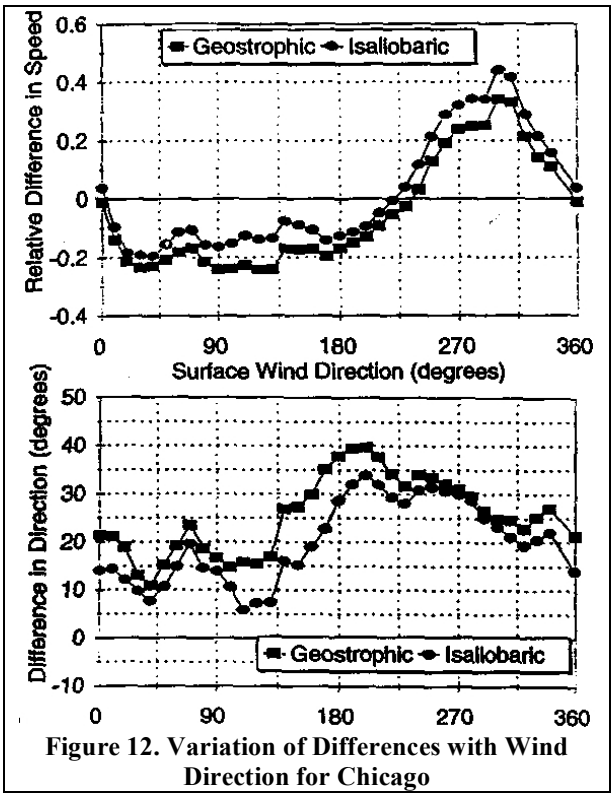

Figure 12. Variation of Differences with Wind Direction for Chicago

It can be seen in Figure 16, that the extreme peaks of both the geostrophic and the isallobaric estimates are, on average, of slightly longer duration than those of the measured windspeeds. This is inconsistent with the peak clustering explanation for a higher crossing rate in the derived windspeeds. More apparent in this figure is the fact that the average time between exceedances is considerably shorter. For example, the average tune from when the windspeed drops below 100 *mph* to when it again exceeds the 100 *mph* threshold is about 900 *hrs* in the isallobaric estimates

but it is on the order of 30000 *hrs* (3.4 *yrs)* in the measured data. But this represents the *average* time. What about its distribution?

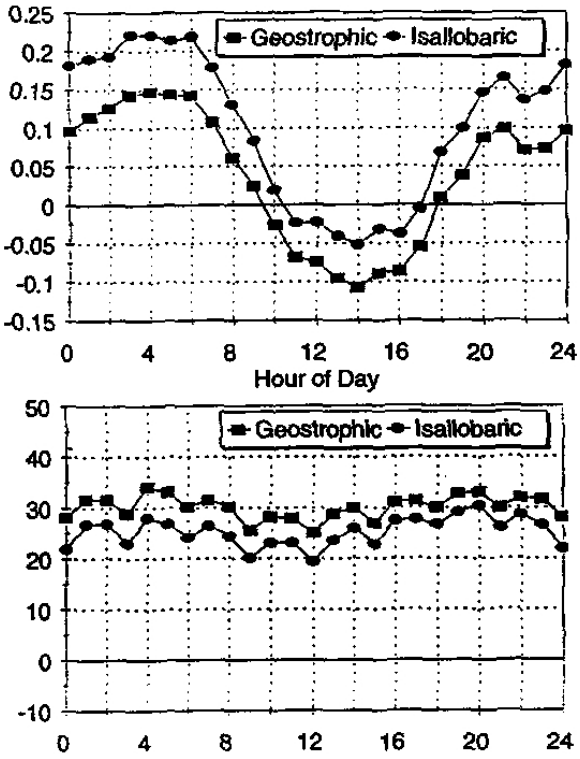

Figure 13. Variation of Differences with Hour of Day for Minneapolis

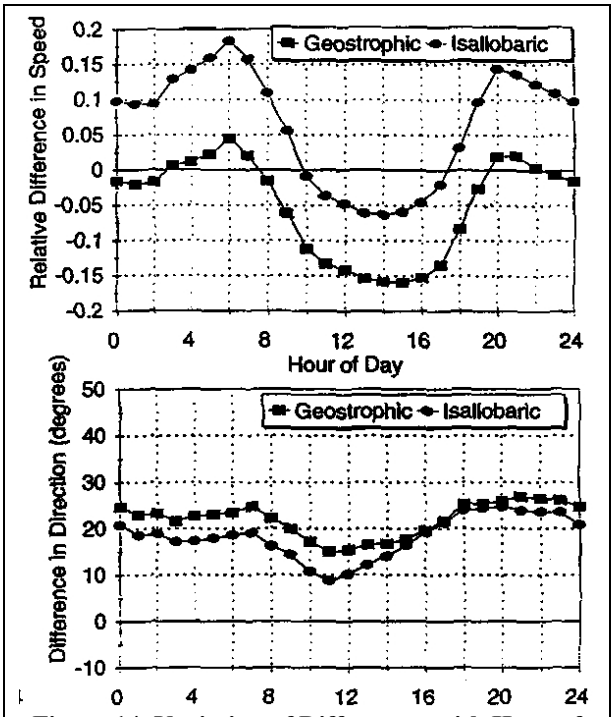

Figure 14. Variation of Differences with Hour of Day for Dayton

Figures 17 and 18 show the actual distribution of times between upcrossings of *80 mph* for each of the processes. In Figure 17, the vertical axis shows the

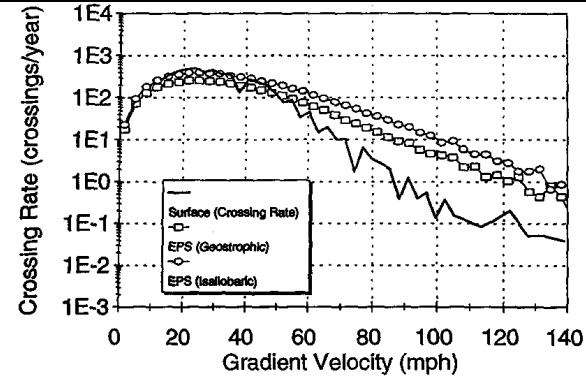

Figure 15. Crossing Rates for Minneapolis

average number of upcrossings per year for which T, the time since the previous upcrossing, is less than a given tune *t.* As t→∞ this value approaches the 80 *mph* crossing rate shown in Figure 15. In Figure 18, each point represents the number of crossings for which the time since the previous crossing fell within a range about t. This shows where the additional crossings of the derived estimates are occurring. While there is some accumulation of crossings in the separation range of 3 - 10 *hrs* for the isallobaric estimate, the majority of crossings fall in the range from 100 - 2000 *hrs.* This confirms that the overestimation of crossing rates is not due to a clustering of peaks, but rather to extra independently occurring peaks.

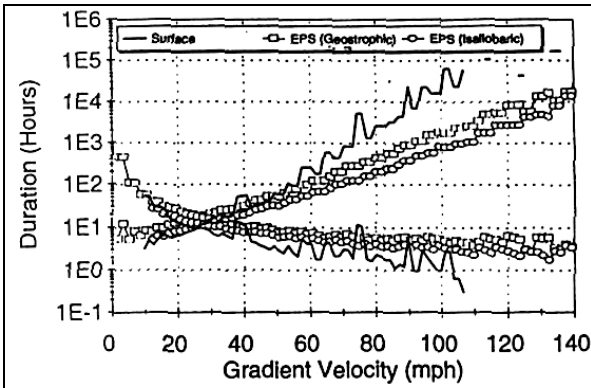

Figure 16. Duration Functions for Minneapolis

Finally, Figure 19 shows power spectral densities of the measured and derived processes. The functions have been multiplied by the frequency *f* and plotted on a log scale in terms of period rather than frequency. This format conserves an area representation of energy. The diurnal periodicity at 24 *hrs* can be seen very clearly in the measured data. (Since the diurnal variation is not purely sinusoidal, there are also harmonic peaks at 12, 8, 6, and 4.8

hrs.) Note that there is apparently no diurnal variation in the pressure field itself. This confirms that the diurnal variations that do occur must result from variations not considered in the derived estimates.

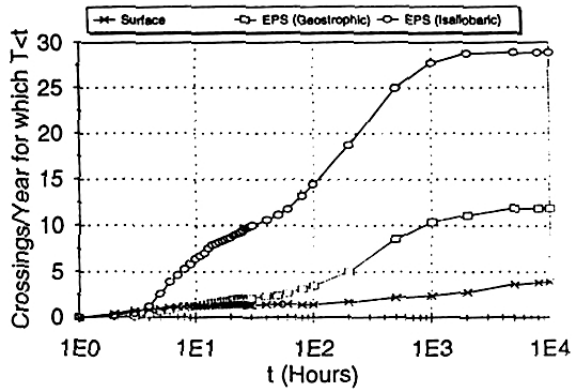

Figure 17. Cumulative Distribution of Times Between Upcrossings of 80 mph

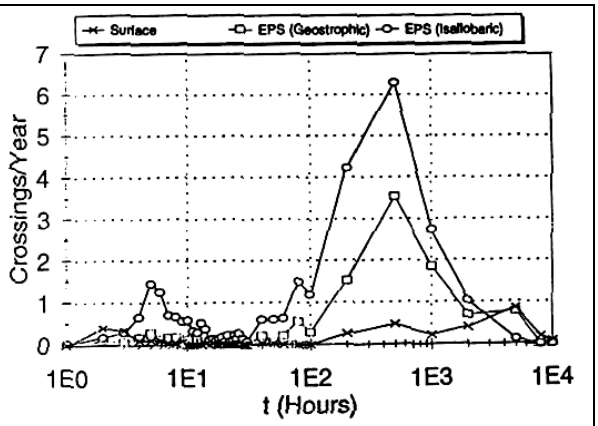

Figure 18. Distribution of Times Between Upcrossings of 80 mph

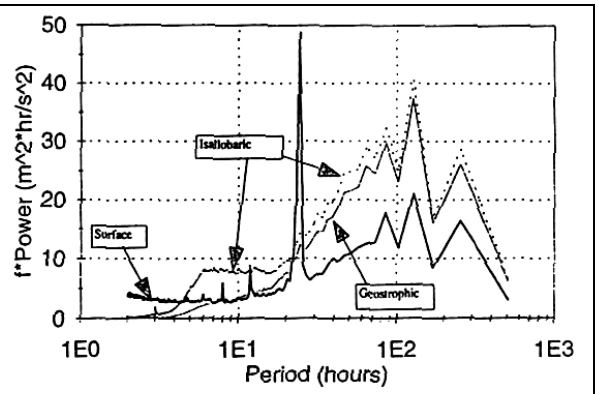

Figure 19. Spectral Energy Distribution for Minneapolis

The effects of the low-pass filtering can be seen in the derived data. Note that there is no low-pass filtering performed on the measured data, so some portion of the apparent high frequency energy is artificial due to aliasing fold-back in the spectral calculation process. It appears that the additional energy in the geostrophic estimates is broadly distributed at periods greater than about 20 *hrs*. The isallobaric estimates contain additional energy particularly at higher frequencies - periods shorter than 20 *hrs*.

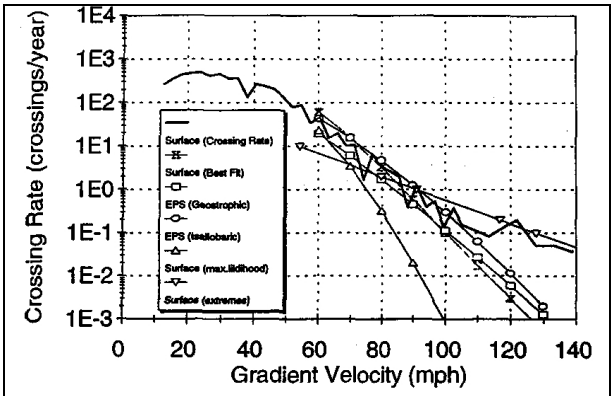

Figure 20. Predicted Crossing Rates for Minneapolis

All of these findings are consistent with the following observations regarding the derived estimates of wind vector time histories using the pressure field approach.

- They contain extra upcrossings, which are not clearly attributable to periodic variations such as diurnal or seasonal.
- These extra upcrossings are, at least in part, due to a sensitivity of the pressure field interpolations to observational errors in the historical pressure measurements, and allowing for some observational error will significantly improve the derived estimates.
- They may be improved further by considering the variations in air density particularly temporal variations (and to a lesser extent, spatial variations).

5 PREDICTED GRADIENT LEVEL WINDSPEEDS

5.1 Modeling of Windspeeds

There two commonly used methods for predicting windspeed as a function of return period in regions not dominated by tropical cyclones. These are the derivation of the extreme windspeeds from the parent distribution of windspeed and direction combined with an upcrossing approach [Davenport, 1983], and the fitting of annual extremes to a Fisher-Tippett Type I extreme value distribution. The upcrossing approach is most commonly used in combination with wind tunnel test data of wind-induced structural responses, whereas the extreme value approach is most commonly used to estimate windspeeds for use

in building codes. A third method is to directly calculate the crossing rate function from time series records; however, this method requires more historical data than is usually available. These three approaches are summarized in the following sections.

5.1.1 Parent Distribution Approach

The analysis of the extra-tropical wind data is undertaken by fitting the hourly data to a Weibull distribution using both directional and non-directional distributions. In the directional case the conditional probability distributions are given in the form

$$P_V(V < v \mid \theta \pm \frac{\Delta\theta}{2}) = 1 - \exp(-(\frac{v}{C(\theta)})^{k(\theta)}) \quad (34)$$

where $C(\theta)$ and $k(\theta)$ are the Weibull parameters describing winds blowing within the section $\theta \pm \Delta\theta/2$. For data obtained from the National Climatic Data Center, $\Delta\theta$ is 22.5° or 10°. By defining $a(\theta)$ as the fraction of time winds blow within the sector $\theta \pm \Delta\theta/2$, the probability of windspeed exceeding *v* within this azimuthal sector is given by

$$P_{V,\theta}(V > v \mid \theta \pm \frac{\Delta\theta}{2}) = a(\theta)\exp(-(\frac{v}{C(\theta)})^{k(\theta)}) \quad (35)$$

and the probability density function is given by

$$p_{V,\theta}(V > v \mid \theta \pm \frac{\Delta\theta}{2}) = a(\theta)k(\theta)\exp\{\frac{v^{k(\theta)-1}}{C(\theta)^{k(\theta)}}\}\exp(-(\frac{v}{C(\theta)})^{k(\theta)}) \quad (36)$$

The probability of exceeding *v* from any directions is given by

$$P_V(V > v) = \sum a(\theta)\exp(-(\frac{v}{C(\theta)})^{k(\theta)}) \quad (38)$$

where the summation is carried out over all sectors. This type of statistical model has been accepted by the wind engineering community as the most reliable method for describing the parent probability distribution for winds associated with extensive pressure system storms, but as described in Twisdale and Vickery [1993], the method is strictly valid only when storms originating from other meteorological phenomena are removed.

The number of occurrences of extreme winds associated with the extensive pressure system storms can be obtained from the parent Weibull distribution of windspeed and direction through the application of Rice's theorem [Rice, 1944] as extended by Davenport [1976]. Under certain assumptions, Davenport showed that the number of upcrossings of a particular windspeed, *v*, is given by

$$N(v) = \left(\sqrt{2\pi}\right)v\sigma_V \sum p_{V,\theta}(v, \theta \pm \frac{\Delta\theta}{2}\Delta\theta) \quad (38)$$

where $p_{V,\theta}$ is the joint probability density function of the velocity *V* and θ, *v* is a cycling rate on the order of 200 to 1000 cycles per year, and σ_V is the variance of the windspeed which is obtained directly from the windspeed data or from the fitted Weibull distribution. The return period associated with the windspeed *v* is given by

$$R(v) = \frac{1}{N(v)} \quad (39)$$

5.1.2 Extreme Value Approach

In the United States, the prediction of windspeeds associated with return periods of 50 or 100 years is most commonly obtained by fitting the annual maximum peak gust or fastest mile windspeed to a Fisher-Tippett Type I extreme value distribution. In most cases, no distinction is made as to what type of meteorological phenomena produced the annual extreme, with the net result being that all extremes are assumed to be produced by events having the same parent probability distribution. Using the extreme value approach, the annual maxima are fitted to the Fisher-Tippett Type I distribution given by

$$P_{\hat{V}}(\hat{V} > v) = \exp(-\exp(\frac{(-v - U)}{\alpha})) \quad (40)$$

where *U* is the mode of the distribution and α is the dispersion. If the directional information is required, then the mode and dispersion become functions of azimuthal sector. Two limitations of the extreme value approach for estimating windspeeds are the influence of local terrain features, structures, and vegetation on the measured winds, and the inability of the approach to readily determine the type of event producing the annual maxima.

5.1.3 Direct Crossing Rate Approach

Both of the previous approaches are employed in order to determine return period windspeeds from limited historical databases. They are essentially short cuts to determining the actual upcrossing rate for extreme windspeeds. The parent distribution approach relies on modeling the windspeed parent process, assuming a strict form such as the Weibull distribution, and then extrapolating to the upcrossing process of the extreme windspeeds of interest. The extreme value approach relies on directly estimating the distribution of extremes based on the available, but often limited, set of historical observations of extreme windspeeds.

The more direct approach of determining the actual upcrossing function of the windspeed process from the recorded data, and then interpolating or extrapolating for the crossing rates at the extreme windspeed range of interest has received less attention. This is in part due to the mistaken belief that the computational effort was significantly greater than that required for modeling the parent windspeed distributions and that the resolution of crossing rate estimate was directly related to the actual number of crossings occurring in the recorded data. In fact, if the recorded data is sufficient to model the parent distributions, and contains enough information to determine rates of change of windspeeds (that is it contains consecutive windspeed measurements over the time scales corresponding to the highest frequency components of the process), then it is also sufficient to estimate the crossing rate function directly. Moreover, extrapolations of the crossing rate, if necessary to reach the extreme windspeeds of interest, are at least as valid as those required for the less direct approaches of modeling distributions where there are more fundamental assumptions involved.

Rice [l944] gave the expression for the upcrossing rate, *N(X),* of a random process, X(t), as

$$N(X) = \int_0^\infty \dot{x} p_{x,\dot{x}}(X,\dot{X}) d\dot{X} \qquad (41)$$

Where $p_{x\dot{x}}(X,\dot{X})$ is the joint probability density function of X and $\dot{X}$. A discrete estimate of the crossing rate function from a discrete process x_i sampled at intervals of Δt, is provided by

$$N_X = \frac{1}{4\Delta x(T-\Delta t)} \sum_{j=1}^{m_x} \left| x_{t+\Delta t} - x_{t-\Delta t} \right| \qquad (42)$$

where m_x is the number of occurrences of $x = X \pm \Delta x/2$ and T is the total length of the discrete time series [Steckley, 1991].

5.2 Comparisons of Predicted Windspeeds

The detailed investigations of the surface level windspeed time histories have resulted in a reasonably good understanding of the characteristics of the current pressure field approach. They revealed some specific improvements, which are required in the current approach before return period windspeeds can be determined directly from the crossing rates of the derived processes. Although these specific improvements have been identified, it is not feasible to perform them within the scope of the present research. We wish, however, to make the best possible estimates of return period windspeeds, given our understanding of the currently derived windspeed processes. Towards this short-term goal, note the following:

- Although, statistically, the mean error of the derived estimates compared to measured data is quite small at high or extreme windspeeds, they overestimate the more common windspeeds.
- Consistent with this, the energy of the derived time history processes is higher over the broad range of frequencies but it is similar in distribution over most of it.
- The crossing rates are in good agreement for low and moderate windspeeds which occur about 95% of the time.

Based on this, the following approach has been taken using test locations of Minneapolis, Chicago, and Dayton. The derived time histories have been scaled so as to reduce the mean error with measured data of the total process to ±4%. A uniform factor of 1.24 provided this correction. The time histories were then converted back to gradient height and the parent distribution approach described in Section 5.1.1 was then used.

Figure 20 shows several results for Minneapolis. First the crossing rate calculated directly from the measured surface windspeeds and converted to gradient is shown. The "Surface (Best Fit)" shows the extreme windspeed crossing rate for this source as determined using the parent distribution approach and a least squares fitting process. This fitting identifies the Weibull model, which best models the data with extra emphasis on the high windspeed data. It represents the best conventionally used fit.

Shown as "Surface (max. likelihood)" are the results for the same approach using a maximum likelihood fitting process instead. This identifies the most probable Weibull model for the data set as a whole.

Consequently this places less emphasis on the high windspeed data and much more on the commonly occurring lower windspeeds.

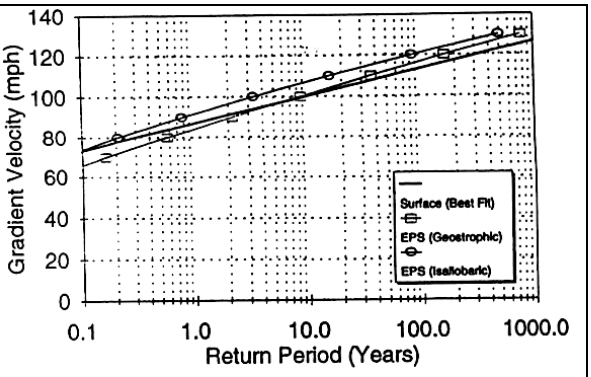

Figure 21. Return Period Windspeeds for Minneapolis

The results using the extreme value approach for the measured data are shown as "Surface (extremes)". This approach is more sensitive to the most extreme data values and a very small number of erroneous data values can significantly affect the result. Consequently, the approach is only used when there is insufficient data to do otherwise.

Finally, the predicted crossing rates for the two derived windspeed processes are shown. These are in reasonable agreement with the best fit of the measured data.

Figure 21 shows the same two results for the derived processes and for the best fit in terms of return period. Figures 22, 23, and 24 show the return period plots for Chicago, Dayton, and Dallas respectively. There is quite reasonable agreement here, considering the known disparities and the approximate approach taken to use the current data in the most appropriate manner.

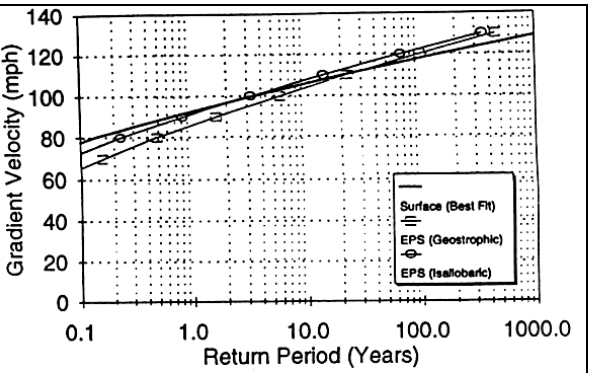

Figure 22. Return Period Windspeeds for Chicago

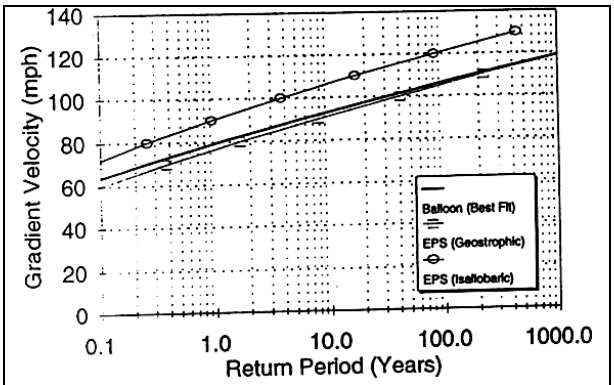

Figure 22. Return Period Windspeeds for Dayton

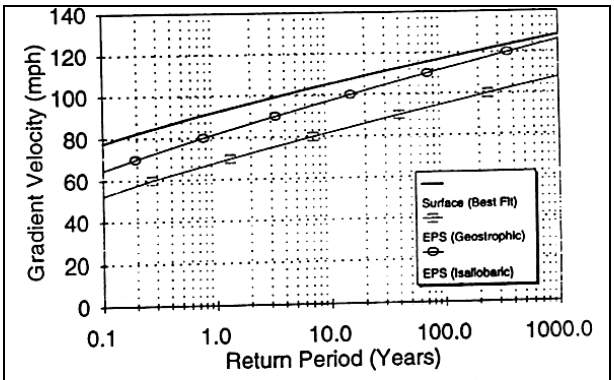

Figure 22. Return Period Windspeeds for Dallas

6 SUMMARY OF FINDINGS

Overall, the new technique developed herein for estimating surface level windspeeds form gradients in the sea level pressure field was remarkably successful. The approach eliminates problems associated with the effects of upstream terrain on surface windspeed measurements and also eliminates problems in extreme wind prediction caused by mixed wind climates. The technique will provide a means to assess the entire area experiencing an extreme wind event associated with the passage of an intense extensive pressure system storm. The following list summarizes the key findings of the study and the main difficulties encountered.

- The set of pressure measurements contained in the NCDC database can be used to reconstruct computer generated pressure fields in a routine manner for any particular hour from 1950 onward. The database is extensive and easily sufficient for the task at hand, but is not uniform in its temporal continuity. Although rare, there are some readings, which contain enough observational error to contaminate the estimates of the pressure field and its gradients using the present interpolation technique. The quality of the reconstructed pressure fields can be significantly improved by a comprehensive patching and reconditioning of the database.

Techniques were developed to identify and remove erroneous data and so the problem can be eliminated in future investigations.

- An approximate expression for the gradient level wind vector can be derived from first principles and expressed in terms of the pressure field, Coriolis parameter, specific volume of the atmosphere (inverse air density), and the temporal and spatial gradients of these quantities. The most significant terms in this derivation are the geostrophic and isallobaric terms. These rely only on the Coriolis parameter, the specific volume, and the first order gradients of the pressure field. Only these terms are investigated in the comparisons of the present work. The next most significant terms are those relying on the spatial gradients of Coriolis parameter and the spatial and temporal gradients of specific volume. It is estimated that these terms may constitute a noticeable but minor fraction of the wind vector estimate. The remaining terms in the derived expressions, specifically those relying on second order gradients of pressure, are estimated to be negligible in all practical cases. (These relative importance calculations are only estimates and could be verified further.)
- Allowing for uncertainties in converting between gradient and surface level winds, the derived wind vectors agree well in overall character and variation with measured data.
- Statistically the derived estimates agree best with measured data values at higher wind speeds (i.e. those important for use in the design of structures and risk analysis).
- Statistically the isallobaric estimate provides an improvement over the geostrophic estimate.
- Diurnal variations in air density, and hence wind velocity, are not accounted for in the present calculations. The windspeed estimates may be improved by including some consideration of these variations.
- Variations in windspeed due to uncertainties in anemometer exposures and related conversions between surface and gradient can be significant. The present work revealed variations at one location (Chicago), which imply apparent underestimates in windspeed on the order of 20% for some wind directions and concurrent overestimates of 30-40% for others. This practical uncertainty confounds reliable comparisons of derived windspeeds with measured data.
- The present calculations tend to overestimate the crossing rates of extreme windspeeds. All investigations herein suggest that this is likely due to observational errors (random precision errors in particular) in the pressure measurement database and the fact that these were not allowed for in the present interpolation technique. This can be easily addressed in Phase II research, but it was not feasible to do so within the scope of the present work.
- Uncertainties in the amount of Ekman rotation of wind direction occurring at specific locations also affect practical conversions between gradient level and surface level wind vectors. The practical consequences of this for determining design wind characteristics are much less than those associated with conversions of windspeed. Nevertheless, further research in this area is needed and will be addressed in the Phase II research.
- Despite the difficulties discussed, it was possible with the present results to make reliable estimates of predicted gradient and surface level windspeeds for return periods from 1 to 100 years. They agree adequately with the best estimates of gradient level return period winds derived from surface measurements, a process which itself contains significant uncertainties. These comparisons relied on judicious application of corrections to account for the identified difficulties of the current windspeed time history derivations. They demonstrate, however, the overall feasibility of the pressure field approach. The improvements and recommendations resulting from the present work will certainly improve these predicted windspeed results in future.

7 RECOMMENDATIONS FOR FURTHER RESEARCH

The following course of action is recommended for Phase 2 research.

- Perform a comprehensive data patching and reconditioning of the NCDC database. First identify and remove those measurements, which are clearly inaccurate or inconsistent with nearby data measurements in space and time. Then fill in all missing data by interpolating from available data in both space and time. Finally, reduce the overall database size, by removing entirely those stations, which are within a minimum distance of other stations, or averaging nearby stations together to form single virtual stations.
- Develop a method that accounts for random precision errors in the individual data measurements by appropriate relaxation in the minimum curvature fitting procedure.
- Investigate the inclusion of additional refining terms in the derived wind vector beyond the geostrophic and isallobaric terms. In particular, those relying on spatial gradients of the specific volume and the Coriolis parameter may offer modest improvements to the estimates.

Alternatively, confirm that they do not warrant the extra effort, and should be neglected.

With these refinements to the overall technique, and with the eventual commercialization of this research effort in mind, it is recommended that the following areas be investigated.

- A major advance made possible by the work presented herein is the ability to assess the size (geographic region) affected by intense extensive pressure system storms. The size of an extreme wind event is needed to estimate the extent of possible wind induced damage, and is extremely important in assessing the reliability of large scale systems such as transmission line networks. The importance of storm size in the assessment of transmission line reliability is discussed in Dagher et al [1993], where it is noted that the current state of the art does not allow for storm size evaluation. The assessment of storm size and region of influence can be evaluated through approaches using auto-correlation techniques (in both spatial and temporal domains). When combined with the EPS models developed herein, one is not restricted to examining correlations between windspeeds at fixed National Weather Stations. One can instead look at an arbitrary grid. Approaches for assessing storm size and damage regions will be discussed in the Phase II proposal.
- Sources of data, which can be used for expanding this geographic domain, should be investigated. In particular expanding northward to include stations from Canada, and southward to include Mexico should be considered. Offshore stations should also be considered.
- Sources of historical pressure data for other continents such as Europe and Asia should be investigated for application of the approach to these locations.

Acknowledgments

The comments and ideas of Dr. F. Lavelle contributed throughout the course of this research and are greatly appreciated.

References

Cook, N. J.; “The designer's guide to wind loading of building structures, Part 1: Background, damage survey, wind data, and structural classification”, Building Research Establishment, 1985, University of Cambridge Press.

Dagher et al, "System Reliability Concepts in Design of Tranmission Lines", *Journal of Structural Engineering*., ASCE, Vol 119, No.l, January 1993, p323-340.

Davenport, A.G., "Discussion of Wind Pressures on Buildings - Probability Densities", BLWT-4-1975 and *Journal of Struct.. Div.*, ASCE, Vol 102, No. ST11, Nov. 1976, p2235-2237.

Davenport, A.G., "The Relationship of Reliability to Wind Loading", *Journal of Wind Engineering and Industrial Aerodynamics,* 1983, 13:3-27

Harris, R.I.; Deaves, D.M. “The structure of strong winds”, *Wind Engineering in the Eighties: Proceedings of the CIRIA Conference held on 12-13 November 1980,* London, Construction Industry Research and Information Association, 1981, Paper 4.

Maddox, R.A., and Bezdek, H.F., "Surface Wind-Pressure Gradient Relationships in Central Florida", *Monthly Weather Review*, November 1994, v122, No.ll, p2596-2602.

Nuss, W.A., and Titley, D.W., "Use of Multiquadric Interpolation for Meteorological Objective Analysis", *Monthly Weather Review*, July 1994, v122, No.7, p1611-1631.

Peterka, J.A., "Improved Extreme Wind Predictions for the United States", *Journal of Wind Engineering and Industrial Aerodynamics,* 1992, 41:533-541

Rice, S.O., "Mathematical Analysis of Random Noise", *Bell Systems Tech. J.*, v!8, 1944, p282; v!9, 1945, p45.

Simui, E.; Changery, M.J.; and Filliben, J., "Extreme Wind Speeds at 129 Stations in the Contiguous United States", B55 118, United States Department of Commerce, 1979, National Bureau of Standards, Washington, D.C.

Steckley, A. and Dalgliesh, W.A., "Statistical descriptions of fluctuating pressures: Field and laboratory investigations", *Progress in Wind Engineering, Proc. of the 8th International Conference on Wind Engineering*, Elsevier 1991, Part I, p!29-140.

Twisdale, L.A., and Vickery, P.J., "Analysis of Thunderstorm Occurrences and Windspeed Statistics", *7th U.S. National Conference on Wind Engineering*, Irvine, CA., June 1993.

Van Miegham, J., "Contribution à l'étude du mouvement de l’air", Académic Royale de Belgique, Classe des Science, Mémoirs, Collection in 8° - Tome XIX, 1941

This page blank